Water Quality Research Journal

Water Quality Research Journal Vol 57 No 4, 247 doi: 10.2166/wqrj.2022.006

Impact of water characteristics on UV disinfection of unfiltered water

Mehrnaz Soleimanpour Makuei*, Faezeh Ketabchi and Nicolas Peleato

School of Engineering, The University of British Columbia Okanagan, 1137 Alumni Ave., Kelowna, BC, Canada V1V 1V7
*Corresponding author. E-mail: mehrnaz.soleimanpour@ubc.ca

MSM, 0000-0002-5328-4487

ABSTRACT

The objective of this study was to examine the impact of unfiltered water conditions on UV disinfection. UV biodosimetry tests were conducted over a year using water samples from two treatment plants that apply UV without filtration. The influence of turbidity, absorbance, and zeta potential on UV dose–response curves was analyzed to evaluate relationships between unfiltered water quality and log-inactivation of surrogate organisms. It was observed that diminishing inactivation with increasing UV dose (tailing effect) was governed principally by the surface charge of particulate matter. The increased tailing level observed in raw waters was postulated to be due to having more neutral surface charges, resulting in elevated electrostatic attraction between particles and microorganisms that increased UV resistance. Inactivation at a dose of 35 mJ/cm^2 in water samples with low turbidity levels (0.38 NTU) and relatively negative surface charge resulted in 3.0 log-removal in comparison with 2.2 and 2.0 log-removal for samples with turbidity levels of 1.57 and 0.61 NTU, respectively. The results of this study highlight the risks of UV disinfection of unfiltered supplies with respect to the effects of water quality characteristics on UV effectiveness and could be employed to optimize the estimation of UV disinfection potential.

Key words: disinfection, small systems, ultraviolet disinfection, unfiltered water, UV-LED

HIGHLIGHTS

- Convectional treatment indicators such as turbidity and UV absorbance (UVA) could not sufficiently interpret the UV disinfection potential in unfiltered drinking water treatment systems.
- Particle surface charge has a more significant impact on UV efficiency than turbidity and UVA.
- Pre-treatments that affect particle surface charge could be used to improve UV disinfection potential of unfiltered sources.

GRAPHICAL ABSTRACT

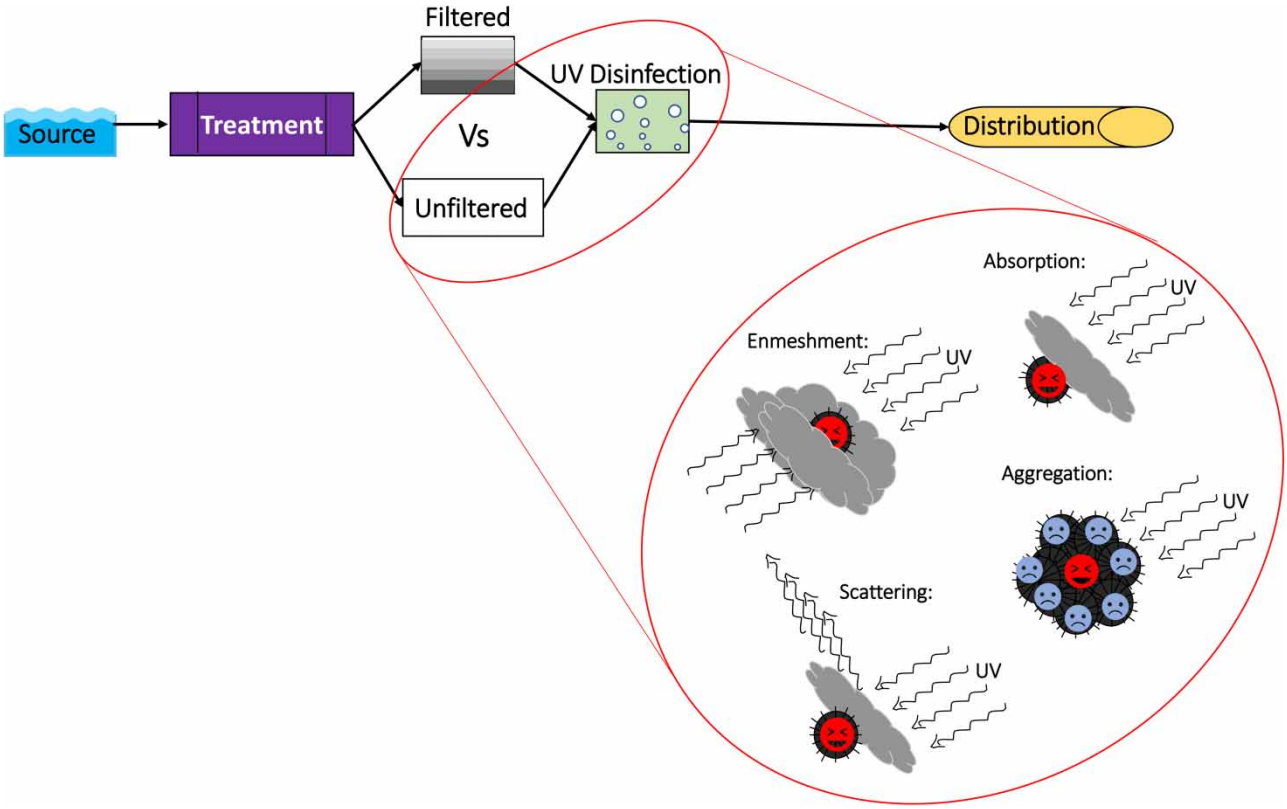

INTRODUCTION

Disinfection is a critical water treatment step applied to eliminate or inactivate pathogenic microorganisms, ensuring that water is safe to drink. Ultraviolet (UV) disinfection is widely used in drinking water treatment and has been growing in popularity since the technology avoids the production of harmful disinfection by-products, does not significantly change water quality, increases operator safety by avoiding oxidants, and is efficient for the inactivation of chlorine-resistant pathogens (Bhullar *et al.* 2019). As a disinfection unit process, UV irradiation is usually applied following a filtration process that reduces concentrations of particulates that may interfere with the exposure of pathogens to UV irradiation. In some cases, it would be desirable to omit the filtration process due to the additional infrastructure that leads to increased cost, maintenance, and footprint (Templeton *et al.* 2008). Guidelines from the USEPA and Health Canada outline criteria to exempt systems from using filtration at any point in treatment (USEPA 2004; Health Canada 2019) if the source water is of sufficiently high quality (either surface or groundwater). Filtration exemption criteria typically include general guidelines in relation to particulate counts and pathogen concentrations, such as influent turbidity levels less than 1.0 NTU and consistently low levels of fecal indicator bacteria, such as *Escherichia coli*, from regular source water quality monitoring (USEPA 2004).

Large-scale systems using source waters that meet exemption criteria may therefore utilize UV for disinfection without prior filtration. Furthermore, UV disinfection without filtration is a particularly attractive technology for small and point-of-use systems due to low maintenance and operational requirements. One of the primary limitations of UV disinfection is the lack of a residual disinfectant, which is more limited of a concern for small systems with small distribution systems (Parrotta & Bekdash 1998). To meet health guidelines, the lack of residual disinfectant could lead to demand for a separate disinfection process which could be of more cost and operational difficulties. Additionally, rapid development and decreasing costs of ultraviolet light-emitting diodes (UV-LEDs) are likely to further increase the use of UV disinfection in small systems due to cost-effectiveness and lower input energy requirements (Chen *et al.* 2017). Economic and operational requirements associated with conventional filtration technologies serve as barriers to small water systems

being able to implement adequate levels of treatment. It is generally not economically efficient to construct and/or operate filtration systems in small water treatment plants, leading to the expectation of many small system UV applications, and in particular UV-LED applications due to its flexibility in design and lower power input, may operate UV without pre-filtration.

Foregoing pre-treatment steps, such as filtration, increases the potential presence of particles in the water entering the UV reactor. UV light can interact with particulate matter in water and be scattered, reflected, or absorbed, leading to the loss of disinfection power (Christensen & Linden 2003). Furthermore, microorganisms can be surrounded, enmeshed, or otherwise shielded by particles. UV disinfection occurs when a sufficient amount of light at the desirable wavelength penetrates through water and is delivered to the target microorganism (Templeton *et al.* 2008). In particle-laden water, the interaction of microorganisms with particles (organic and inorganic) and flocs (biological and chemical) could offer them survival from the disinfection stage. Previous work has identified inactivation of microorganisms by UV light typically has an increasing log-linear trend up to a certain dose, after which the application of additional UV light energy results in a limited increase in disinfection. This plateau or tailing effect is thought to be due to a fraction of the microorganisms that are resistant to UV disinfection, possibly due to being shielded by particulate matter or aggregation of organisms into clusters providing some degree of protection (Tan *et al.* 2017). Tailing effects are important to consider in order to understand the effect of water source-specific characteristics on the required UV dose and energy to achieve the desired level of disinfection. Particles could also lead to an overestimation of the delivered UV dose, where the UV dose or intensity measured does not consider the effect of reflected light from the surface of particles.

Previous studies have shown that the physical and chemical properties (size, concentration, surface charge, hydrophobicity) of particles present in water are crucial factors in microorganism–particle association (Cantwell & Hofmann 2008; Templeton *et al.* 2008). Furthermore, particle association and aggregation strength can be influenced by the characteristics of the organisms (Farrell *et al.* 2018). Numerous efforts have been made to define relationships between particle size and UV disinfection efficiency. A wide range of critical particle sizes, or sizes at which a particle is large enough to effectively shield microorganisms from UV light, have been reported. Critical particle sizes are likely influenced by differences in particle and microorganism characteristics, reflected in variability in previous reported influential ranges of 7–11 μm (Cantwell *et al.* 2010), 11–25 μm (Kollu & Örmeci 2012), and 263 μm and larger (Winward *et al.* 2008).

Dose–response modeling of UV behavior is important for system design and assurance of expected performance as water quality characteristics change. Previously reported models and UV disinfection equipment dose calibrations complying with the UV Disinfection Guidance Manual (UVDGM) generally account for UV absorbance (UVA) or UV transmittance (UVT) as the only and most influential process quality control (Wright *et al.* 2011). The accuracy of the mentioned statement was validated by Tan *et al.* (2017) who successfully developed a model for quantification of the impact of dose and UVA on tailing phenomena. However, the results presented by Farrell *et al.* (2018) demonstrated that UVA or UVT, or turbidity could not explain the observed dose–response. Water samples with equal UVA or turbidity but with particulates with unique compositions showed unexpected behavior after UV exposure. Turbidity does not offer information on particle characteristics, such as surface charge, that may directly or indirectly impact the UV response. For instance, if an organism–particle association is a major driver of tailing effects, the surface charge of the organism and the particle will define the degree of electrostatic attraction and largely dictate the strength and probability of shielded organisms (Farrell *et al.* 2018).

There is currently limited guidance and knowledge on acceptable water quality conditions when applying UV disinfection to unfiltered water supplies. As such, there are concerns about the application of UV disinfection in water systems meeting filtration exemption criteria or for small systems. Furthermore, previous research has highlighted that particle characteristics, such as surface charge, play a crucial role in the resulting disinfection response; however, they have not been incorporated into dose–response modeling. This study aims to identify water quality characteristics of unfiltered systems that may impact UV disinfection and to suggest critical water quality characteristics that may need to be monitored to estimate disinfection achieved. Biodosimetry tests using samples from two water treatment facilities that operate UV disinfection systems without filtration were obtained over 1 year. The impact of different particles at different concentrations on UV disinfection efficiency is discussed, and a relationship between the water quality parameters and treatment indicators UVA, UVT, turbidity, zeta potential, and UV dose–response is developed.

METHODS

Water samples preparation

Grab samples of water were taken immediately prior to the UV disinfection process at two full-scale water treatment plants located in Vernon and Lavington, BC, Canada, respectively: Duteau Creek Water Treatment Plant (DCWTP) and Mission Hill Water Treatment Plant (MHWTP). Additionally, a sample of untreated intake water from DCWTP was used (referred to as DC raw) to represent no treatment. Since no treatment is applied before UV disinfection at MHWTP, no additional sample was needed to represent intake water. Samples were collected monthly from October 2020 to August 2021. The water samples were collected in dark glass bottles to prevent photoreactivation and were sanitized and pre-washed with the source water before sampling (Crittenden *et al.* 2012).

500 μL of MS2 stock (at a concentration of 10^{10} PFU/mL) were added to 19.5 mL of grab samples for UV exposure experiments. Then, samples were mixed (magnet stirrer at 50 rpm) for 30 min to encourage potential particle–microorganism association. The UV dose–response experiments were carried out for each sample at the time of collection in triplicate and the inactivation curves were generated from the average of the replicates. Particle size distribution (PSD) and zeta potential (ζ) were measured using a Zetasizer Nano ZS (Malvern Instruments, Ltd, Westborough, MA). UV light absorbance of water samples (UVA) was measured using HORIBA Scientific Aqualog spectrometer (Piscataway, NJ). A VWR Turbidity Meter was used to measure sample turbidities, and pH measurement was carried out using a Thermo Scientific Orion 3-Star Benchtop pH Meter. Total organic carbon (TOC) was quantified using a Shimadzu TOC-L. The UV light intensity was measured using an ILT2400 Optical Light Meter to determine the UV dose delivered. All measurements were taken in triplicate to check the repeatability of the results obtained.

Fluorescence analysis was also conducted to characterize natural organic matter. Samples were first filtered through a 0.45 μm filter and then fluorescence intensities at iterated wavelengths were collected using an Aqualog spectrophotometer (HORIBA Scientific, Piscataway, NJ). Wavelength ranges collected were from 240 to 400 nm at 5-nm increments (excitation) and 280 to 500 nm at 2-nm increments (emission). Inner filter effects were corrected internally by the instrument using an absorbance spectrum that had been acquired at the same time. Intensities were blank subtracted using type 1 water, and then normalized to the blank water Raman peak at 370 nm excitation. PARAFAC analysis was applied using the drEEM toolbox for MATLAB and following the methodology reported by Murphy *et al.* (2013). The number of PARAFAC components in the finalized model was determined by observing conformity to general theoretical guidelines on how the fluorescence from individual organic components should appear, such as only one emission peak. Furthermore, the number of components was confirmed by split-half validation, where the consistency of extracted components in randomly selected dataset halves is verified.

Microorganisms propagation and MS2 assay

Based on the size, structure, and surface charge of enteric viruses and *Cryptosporidium*, MS2 with a small size of 25-nm diameter and a negative surface charge was determined to be an acceptable surrogate for a UV-based disinfection method. Therefore, Male-Specific MS2 bacteriophage was used as a conservative surrogate for Cryptosporidium (MaCkey *et al.* 2002). Freeze-dried vials of *E. coli* bacteriophage MS2 (American Type Culture Collection (ATCC) 15597-B1) and its host *E. coli* (ATCC 15597) were rehydrated and propagated following their respective ATCC product sheets. To culture *E. coli*, LB broth (Miller formulation; Fisher Scientific) was chosen as media for host bacteria. 10 mL of LB was inoculated with 20 μL of frozen *E. coli* and grown overnight at 37 °C. 50 mL of fresh LB was then inoculated with 1 mL of overnight cultured *E. coli*, followed by incubation at 37 °C with continuous shaking at 100 rpm to obtain a culture in its log growth phase. All water samples containing MS2 phage were serially diluted using an LB broth medium. Then, 50 μL of host cell solution, 0.1 mL of diluted MS2 phage sample, and 2–3 mL of molten soft agar (0.6% agar, 40–45 °C) were combined. The mixture was then poured onto the solidified 1.5% agar in petri dishes. After hardening the top layer of agar, plates were covered and incubated upside down for 16–24 h at 35–37 °C. Observed plaques identified as clear circular zones were counted, multiplied by the dilution factor, and divided by the sample volume in milliliters to determine the titer in plaque-forming-unit per mL (PFU/mL). According to USEPA, log-inactivation values of MS2 should be multiplied by 1.77 to represent Cryptosporidium log-removal (Pirnie *et al.* 2006).

UV inactivation experiments

A UV-LED system consisting of multichip arrays of UV-LEDs enclosed in a glass housing (PearlLab BeamTM, AquiSense Technologies) was used to carry out inactivation experiments. Water samples containing MS2 were irradiated under LEDs

at a wavelength of 256 nm with an average intensity of 478 μW/cm^2, measured using an ILT2400 radiometer (International Light Technologies). A petri dish with a 70 mm diameter containing 20 mL of solution (comprising a water sample and MS2 bacteriophage) was placed under the LEDs, and the complete petri dish was illuminated. In all experiments, samples were exposed to four different doses from which 20 μL of the sample was taken at each dose level to conduct serial dilution and MS2 enumeration. All dose–response measurements were taken in triplicate from the grab samples (20 L) taken from each sampling position and exposed to UV disinfection.

UV inactivation kinetics of bacteria

The reduction in the abundance of bacteriophage (N_0) due to UV exposure can be described by a double-exponential model as follows (Tan *et al.* 2017):

$$N = (1-\beta)N_0 e^{-k_1 UV_{Dose}} + \beta N_0 e^{-k_2 UV_{Dose}} \quad (1)$$

where N is the residual number of culturable MS2 after UV exposure in PFU, N_0 is the initial number of culturable phages in PFU, and D is the delivered UV_{Dose} in mJ/cm^2. In addition, β indicates the fraction of UV-resistant phages, and finally k_1, and k_2 represent first-order inactivation rate constants for UV-susceptible and UV-resistance fractions, respectively. The use of a double-exponential model allows for the representation of tailing effects, or concavity to the dose–response model, that are commonly observed from UV disinfection.

UV_{Dose} delivered to the sample is calculated using the following equation (Pirnie *et al.* 2006):

$$UV_{Dose} = E_s P_f (1-R)\frac{L}{d+L}\frac{(1-10^{-A_{254}d})}{A_{254}\, d \ln(10)} t \quad (2)$$

where E_s is the average UV intensity (measured before and after irradiating the sample) (mW/cm^2); P_f is the Petri Factor (unitless); R is the reflectance at the air–water interface at 254 nm (unitless); L is the distance from lamp centerline (cm); d is the depth of the suspension (cm); A_{254} is the UV absorbance at 254 nm (unitless); t is the exposure time (s).

The average UV intensity was calculated from the measured UV intensity incident on the surface of the microbial suspension using the light meter. Reflectance (R) at the air–water interface can be calculated using Fresnel's Laws as 0.025. In addition, the Petri Factor term compensates for the fact that the irradiance is not uniform over the entire surface area of the sample container. To calculate this factor, the average irradiance across the sample surface was determined by measuring irradiance at specific distances from the center of the petri dish along two perpendicular lines. The ratio of the average irradiance to the center irradiance determined the Petri Factor, which was measured as 0.99 for the experimental setup used in this work (Zimmer & Slawson 2002). The distances from the lamp centerline (L) and depth of suspension (d) were equal to 9.4 and 0.52 cm in the experiments, respectively.

Statistical analysis

The statistical significance of the results was investigated using Student's t-test. It was performed in pairs for the β, P, k_1, and k_2 terms of the double-exponential model at a 95% confidence level. The difference between the two samples was deemed to be statistically significant if the calculated p-value was ≤ 0.05.

RESULTS AND DISCUSSION

Water quality characterization

Three sources of unfiltered water were used in this study with varying levels of treatment. Two sample locations (DCWTP and MHWTP) are directly upstream of UV disinfection at the two water treatment plants. However, no filtration process has been applied in either case. Before UV disinfection at DCWTP, raw water is treated by a dissolved air flotation (DAF) process using poly aluminum chloride and coagulation and flocculation aid (Epi Amine and Hydrofloc). There is no treatment prior to UV at MHWTP, and therefore the MH pre-UV sample is also representative of unfiltered source water characteristics in Kalamalka Lake. For this study, the experimental design was to focus on a periodic sampling of pre-UV water at two large-scale plants that do not practice filtration. An additional raw water sample was included to expand the range of water quality tested and help elucidate the potential effects of water quality on UV disinfection. Sampling was carried out

over a year to capture seasonal changes in water quality and provide an overall assessment of the UV disinfection performance at the two unfiltered facilities.

Water characteristics (turbidity and pH) were recorded during the sampling period from October 2020 to September 2021. Figure 1(a) shows that pre-UV samples were consistently below 1.0 NTU up to August 2021. An increasing trend in the turbidity of two non-treated water samples (MH pre-UV and DC raw water) in summertime (July–August 2021) could be attributed to several possible factors such as recreational activities, or the increase in the water temperature causing calcite precipitation (Korchef & Touaibi 2020; Schafft *et al.* 2021). It should be noted that the risk pathways could be different for the two sources because MHWTP is prone to calcite precipitation and DCWTP source water is characterized as an upland watershed influenced by rainfall and runoff and with recreational, forestry, and grazing activities within the watershed. Due to the pre-treatments at DCWTP, the turbidity of pre-UV samples was consistently below 1.0 NTU, while the turbidity of DC raw water samples varied between 1.1 and 3.5 NTU. The observation of specific periods of elevated turbidity during the sampling period implies the importance of understanding the impacts of turbidity on UV disinfection and the need for a reliable method to ensure adequate delivery of UV dose.

Further to the possibility of turbidity impacting the UV disinfection process, elevated turbidity is often used as a surrogate for increased microbial contamination of sources. Weak relationships between turbidity and coliform counts ($R = 0.14$), as well as with *E. coli* ($R = 0.17$) were observed on sampled days, suggesting spikes in turbidity did not imply increased microbial concentration in the source. However, it should also be considered that coliforms and *E. coli* counts are non-precise indicators of protozoa presence (Lalancette *et al.* 2014).

UVA was recorded during the sampling period from October 2020 to August 2021. UVA at 254 nm is reported at two scales for all water samples in Figure 1(c). Both pre-UV samples showed similar trends and consistently low levels of absorbance (0.07 absorbance, 85% transmittance), implying a high degree of UV light penetration through the water. DC raw samples were more colored, reflected by an average UVA of 0.35 with a maximum of 0.50 in April 2021. TOC was recorded over a subset of the sampling period (February 2021–August 2021) due to instrument limitations. TOC results showed similar trends for all water samples and varied between 7.46 and 11.83 mg/L, 3.68 and 4.64 mg/L, and 3.65 and 4.13 mg/L for DC raw, DC pre-UV, and MH pre-UV, respectively. The large spike observed in turbidity and TOC in the spring for DCWTP pre-UV and raw water could be indicative of freshet conditions and increased organics in the source water. The ascending trend in turbidity was not reflected by TOC measurements for MH pre-UV water samples from July 2021 to September 2021. Since TOC would capture changes in particulate organic concentrations, the proportion of particulate matter that resulted in the spike in the turbidity at the last three sets of sampling was more likely due to changes in inorganic particulate material present in the MH source.

Fluorescence spectra of water samples were recorded to characterize the dissolved organic matter and as an indicator of water matrix diversity. PARAFAC analysis was applied to the fluorescence spectra to identify underlying humic-like and protein-like signals (Murphy *et al.* 2014a). A four-component model was split-half validated and the corresponding extracted components are presented in Supplementary material. To assist in identifying the identity of the extracted components, the validated model was cross-referenced with the OpenFluor database (Murphy *et al.* 2014b). The extracted components, references to similar components, and possible identity are presented in Table 1.

The component scores, reported as F_{max}, are shown in Figure 2. Generally, it was observed that humic-like fluorescence (C1–C3) was more variable in water samples from a creek source (DC) as compared to a lake (MH pre-UV/raw) over the sampling period. Previous work has suggested an emission threshold of 450 nm to help differentiate between carbon oxidation generally above and below 0 (Lavonen *et al.* 2015). DC raw and DC pre-UV had a greater proportion of fluorescence with emission above 450 nm (average over the study period: DC raw 50.8 $\pm$ 1.1%, DC pre-UV 44.5 $\pm$ 2.7%) compared to MH pre-UV (34.3 $\pm$ 2.9%), suggesting an overall greater proportion of oxidized carbon in DC samples. A less pronounced difference in protein-like F_{max} between DC raw and pre-UV samples was observed. Furthermore, pre-treatment at the DC facility (DAF) generally resulted in lower removal of protein-like fluorescence (–96.3% increase to 74.4% removal), compared to humic-like components (4–88.3% removal for C1–C3). The fluorescence results suggest that the organic characteristics are unique to the three samples in this study.

Drinking water contamination has caused numerous waterborne disease outbreaks, even in countries with sophisticated treatment systems (Muoio *et al.* 2020). Different species of protozoa are prevalent in surface and groundwater, and they can exist in a dormant oocyst form that is resistant to environmental effects until the proper host is available. The potential for pathogen transmission during UV disinfection implies the importance of a full assessment of disinfection efficiency when

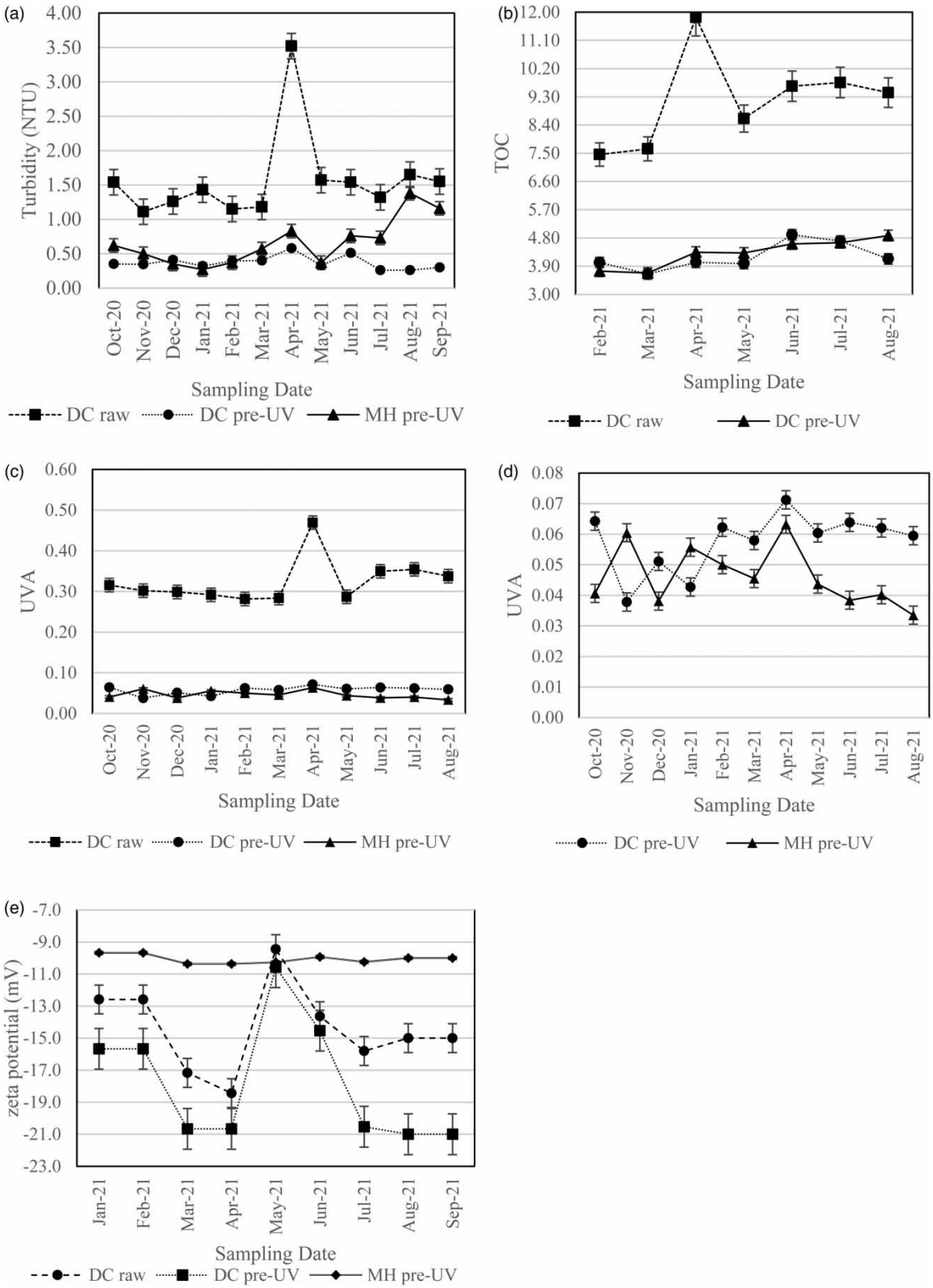

Figure 1 | (a) Turbidity over the 1-year sampling period, (b) TOC from February to August 2021, (c) average UV absorbance at 254 nm, (d) UV absorbance of pre-UV samples, and (e) sample date vs. zeta potential of grab samples. Values are the average of triplicates, and vertical error bars represent one standard deviation.

Table 1 | Fluorescence components identified by PARAFAC and comparison results from the OpenFluor database

Component	Excitation/Emission maximum(s) (nm)	Description and possible identity	References (>0.98 similarity score in OpenFluor)
C1	Ex: ≤ 250, 340 nm Em: 470 nm	Terrestrial humic-like; soli-derived fulvic acid	Kowalczuk *et al.* (2009) (C1) Osburn *et al.* (2016) (C1) Garcia *et al.* (2018) (C1) Du *et al.* (2021) (C4)
C2	Ex: ≤ 250, 315 nm Em: 405 nm	Microbial humic-like	Kowalczuk *et al.* (2009) (C3) Osburn *et al.* (2016) (C2) Du *et al.* (2021) (C2)
C3	Ex: ≤ 250 nm Em: 420 nm	Terrestrial humic-like	Kowalczuk *et al.* (2009) (C2) Peleato *et al.* (2017) (C2) Jutaporn *et al.* (2022) (C3) DeFrancesco & Guéguen (2021) (C4)
C4	Ex: 275 nm Em: 335 nm	Protein-like/tryptophan-like	Moona *et al.* (2021) (C5) Peleato *et al.* (2017) (C5)

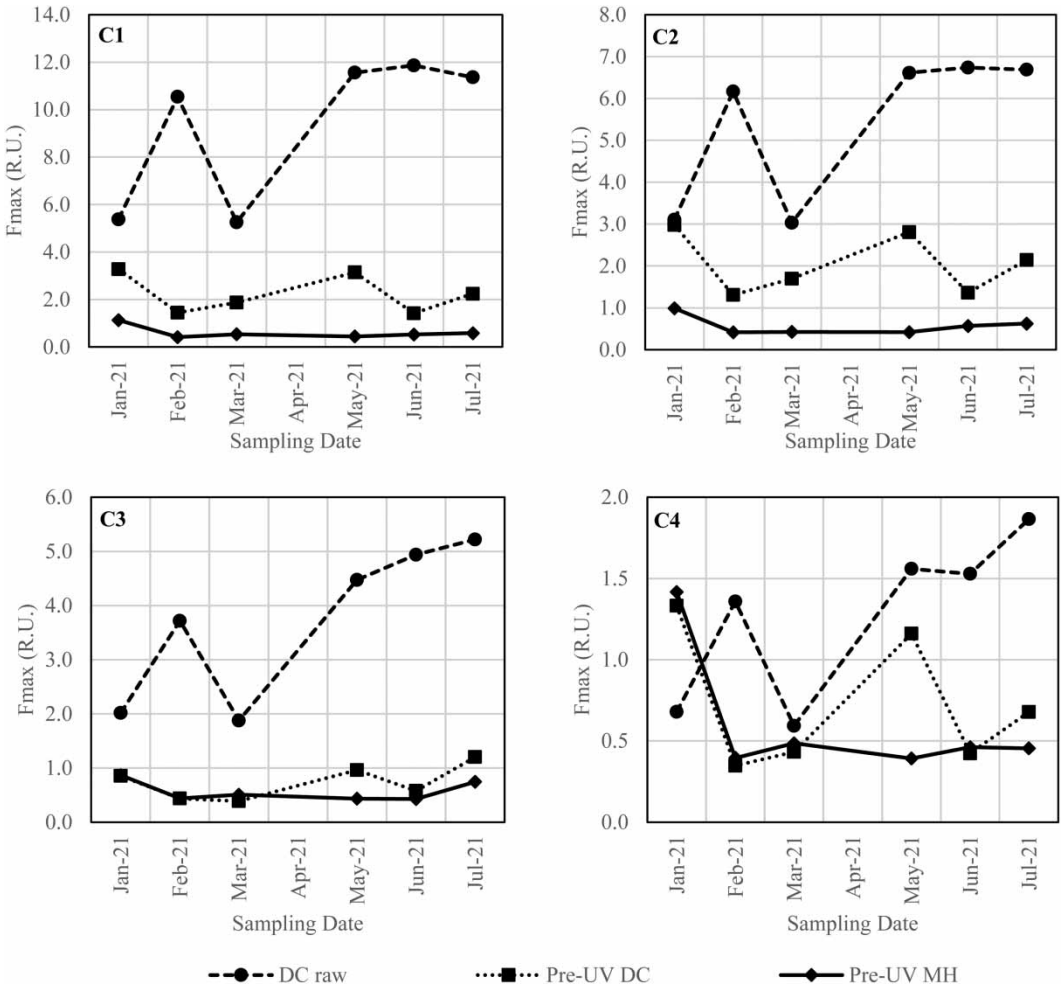

Figure 2 | Scores (F_{max}) of fluorescence components identified by PARAFAC analysis.

facing drinking water contamination risks. Turbidity is often used as the regulatory and operational indicator of increased risk of elevated pathogen levels in drinking water sources. Figure 3 presents the relationship between DC raw water's bacterial contamination (total coliform bacteria and *E. coli* population) and the turbidity trend during the sampling period. The

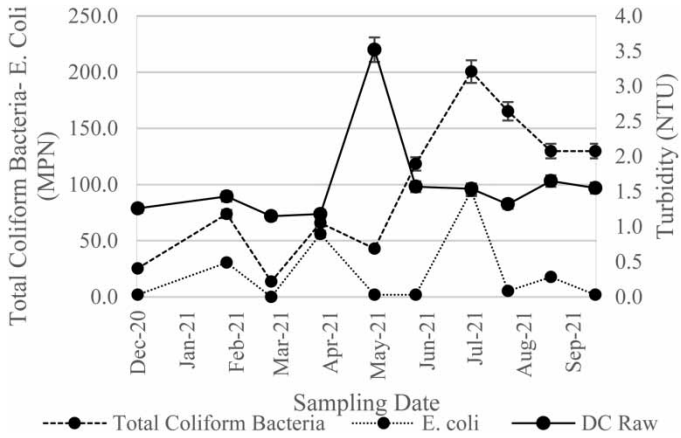

Figure 3 | Turbidity and bacterial concentration of DC raw water during the sampling period.

peak in total coliform bacteria and *E. coli* (June 2021) is not concomitant with the peak in turbidity (April 2021). Additionally, fluctuation in the concentration of microorganisms is seen from December 2020 to June 2021, while the turbidity remained constant at 1.3 ± 0.17 NTU. Turbidity could not reflect the associated risk of changing source water pathogen concentrations in the drinking water treatment plant influents.

Zeta potential was recorded during the sampling period from January 2021 to September 2021. Zeta potential represents the electrostatic potential at the electrical double layer around a particle in solution. As presented in Figure 1(e) in MH pre-UV, particle surface charges were more neutral ($\zeta = -10.4 \pm 1.9$ mV) than DC raw water ($\zeta = -17.2 \pm 2.1$ mV) and DC pre-UV ($\zeta = -20.9 \pm 0.9$ mV). MS2 and Cryptosporidium are expected to be negatively charged in water, with potentials of approximately −27 to −35 mV, respectively. It was hypothesized that if microorganism–particle association drives tailing effects, samples with less negatively charged particles in MH pre-UV and DC raw water would experience greater tailing effects due to greater attractive forces between MS2 and particulates. According to Figure 1(e), the changes in zeta during the year are analyzed. Zeta potential is constant in MH pre-UV samples despite no treatment. However, treatment at DCWTP consistently makes the average particle charge more negative. The difference between DC raw and DC pre-UV is more pronounced during specific times of the year and could be due to treatment changes. Runoffs introducing freshets to DCWTP could also be responsible for the abrupt change from May to June 2021.

Average inactivation

Grab samples were collected once a month at three sampling locations. The average UV inactivation of each sample over the year was calculated using the data collected from December 2020 to September 2021 (Figure 4). The exposure times were selected to be constant during all experiments at 15, 25, 80, and 100 s, and doses were corrected based on water quality, as explained in Methods. The observed results suggest that any additional energy over 30.0 mJ/cm^2 does not increase inactivation significantly and may not be worth the associated costs ($p > 0.05$ in all water samples, $n = 11$). Control experiments (distilled water with no particulates) showed higher log-inactivation (Figure 4) and presented a similar plateau effect at UV doses above 30 mJ/cm^2. This indicates that water quality does prevent disinfection from reaching the maximum possible reduction (disinfection in control samples is higher). However, tailing effects occur to some extent even without particulates or other components in the water. This is likely due to the aggregation of organisms that could have survival effects on microorganisms. The initial phage concentration in conducted experiments was 108 PFU/mL. Thus, the plateau obtained after 30.0 mJ/cm^2 cannot be attributed to the complete inactivation of MS2. Dose–response curves begin to separate above 20 mJ/cm^2, and at 30 mJ/cm^2 DC pre-UV shows a notable increase in inactivation compared with the other two. There is a statistically significant improvement in average log-removal in DC pre-UV samples compared to DC raw water and MH pre-UV samples at 30 mJ/cm^2 (1.2 log improvement) and 50 mJ/cm^2 (1.1 log increase) ($p < 0.001$). As such, it can be concluded that tailing is present in all sample types after approximately 30.0 mJ/cm^2; however, treatment at DCWTP does significantly improve average log-inactivation at higher UV doses.

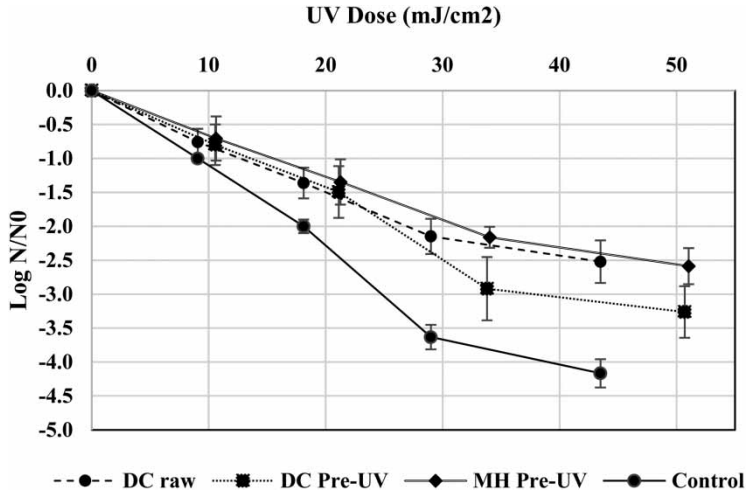

Figure 4 | The average dose–response curve of MH, DC pre-UV, and DC raw calculated from December 2020 to September 2021 under a UV wavelength of 254 nm with four different UV doses. Control tests are representative of MS2 inactivation in reverse osmosis water. Doses are variable based on corrections to estimate the actual dose delivered; exposure times were constant for all tests. Error bars represent one standard deviation ($n = 8$–11).

Pre-treatment at the DCWTP (coagulation, dissolved air filtration) is likely the cause of the observed difference at high UV doses. Figure 5 presents log-removal values normalized by sample turbidity (a), UVT (b), zeta potential (c), and UVA (d). The intention was to identify if dose–response curves would look similar when accounting for the impact of water quality characteristics in different water samples. To analyze the consistency of the values in the transformed dataset, the level of dispersion was also indicated from the coefficients of variance around the mean.

Figure 5 shows that turbidity or UVA independently does not explain the variability in average log reduction identified in Figure 4. A successful normalization factor would be expected to result in equal responses between water samples. In all cases, each water source was observed to have a statistically significant difference in normalized log reduction for all exposure times ($p < 0.001$). Cantwell & Hofman (2011) concluded the same results while investigating the absorption properties of suspended particle matter in untreated water (Cantwell & Hofmann 2011). Monitoring of turbidity and UVT in unfiltered waters to determine the disinfection potential may not accurately reflect the actual UV disinfection efficiency.

When normalized by surface charges, the effect of different surface charges is minimized in dose–response curves of MH pre-UV (no treatment before UV) and DC raw water compared to the other figures. However, significant differences remained between log-inactivation for each water source at any given exposure time ($p < 0.008$). It is worth noting that the MHWTP surface charge remained relatively constant throughout the study period, whereas the DCWTP raw and pre-UV samples varied seasonally as the raw water characteristics changed.

Normalization by surface charges resulted in reduced variability between log-inactivation between sampling dates as opposed to normalization by turbidity and UVA in each sampling position. There was a pronounced increase in the dispersion of the data when normalized by turbidity and UVA. For DC pre-UV water samples, the average coefficient of variation over sampling days increased from 22.6% (no normalization) to 114.3% when normalized by turbidity and 23.3% (normalized by UVA). MH pre-UV results showed similar trends with the average coefficient of variation in monthly data increasing from 22.0 to 51.2% (normalized by turbidity) and 30.5% (normalized by UVA). For both DC and MH pre-UV samples, normalization by zeta potential decreased variation to 18.8 and 17.3%, respectively. A decrease in month-to-month variation in dose–response when normalized by zeta potential suggests this measure captures some degree of variability and is valuable to an overall assessment of expected UV inactivation levels.

It appears that based on the data collected, particulates' surface charge explains some degree of dose–response variation within the two untreated natural water samples that were the most and least turbid samples. However, it did not account for the other water source that experienced treatment (DC pre-UV). The increase in negative surface potential of particulates from DC raw water to DC pre-UV was unexpected since coagulation should cause neutralization of surface charges and shift zeta potentials towards 0 mV. It is possible that through the dissolved air floatation process, the fraction of particulates that

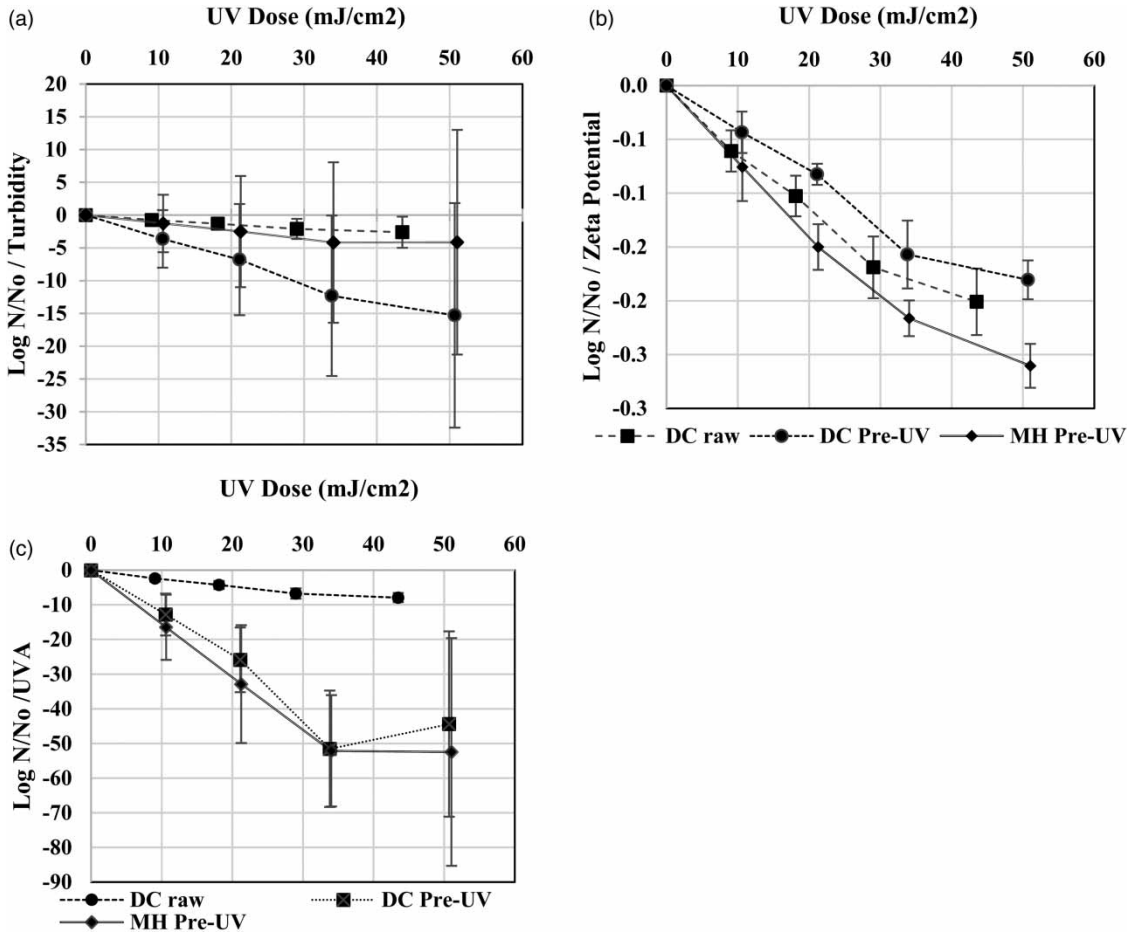

Figure 5 | Average log-inactivation normalized by (a) sample turbidity, (b) zeta potential at average pH 7.2, and (c) UVA.

were neutralized were removed in flocs, while another fraction remained and was not effectively removed by treatment. Due to electrostatic attraction, in the presence of neutral particles and microorganisms with a negative surface charge (−27 to −35 mV), the aggregation of microorganisms and particles was more likely to happen and therefore, microorganisms were trapped and became shielded from UV, and contributed to higher levels of tailing. As observed in Figure 4, the average inactivation of MH pre-UV water samples, containing particulates with the least negative surface potential, reached a plateau after 2.0 log-removal as opposed to 2.5 and 3.5 in DC raw and pre-UV samples, respectively. This is in agreement with results observed by Farrell *et al.* (2018) where chalk and Fe^{3+} with zeta potentials of −3.5 and −3.9 mV were associated with higher levels of tailing as opposed to humic acid and clay with zeta potentials of −13.9 and −17.2 mV at pH 7, respectively. Results obtained provided further supporting evidence for higher levels of particle–microorganism attachment in water samples with more neutral surface charges (Farrell *et al.* 2018). In general, the dose–response curves acquired using the normalized data by surface charge are more representative based on the lower coefficients of variances of the repetitive measurements.

The effect of particles on UV-resistance and tailing

The double-exponential model (Equation (1)) was used to describe the UV inactivation kinetics of water samples. This model was initially developed for UV disinfection of bio-flocs and is repurposed in this study under the premise that microorganisms in the presence of particles, flocs, or aggregated organics can be shielded by being embedded in the suspended particles. Numerous studies conclude that the disinfection of microorganisms is comprised of two stages that are attributed to two different groups of microorganisms (Tan *et al.* 2017). The expectation is that the portion of free-floating microorganisms is prone to be disinfected easily, with the remaining portion that is attached to, enmeshed in, or associated with particles, flocs, agglomerations of microorganisms, and organic matter resulting in the majority of tailing effects. Control experiments

were also conducted on microorganisms with no particles and reverse osmosis water (Figure 1(e)). Complete inactivation is not observed in control samples, and a slight degree of UV-resistance was also detected, which can be connected to the microorganism aggregation. Similar results were observed in previous studies (Farrell *et al.* 2018).

Average values of k_1, k_2, and β fitted from inactivation levels are presented in Table 2. The degree of tailing is captured in the β term. As expected, the percentage of UV-resistant microorganism (β) is significantly different in DC raw and pre-UV with values of 64 and 19%, respectively ($p < 0.001$). DC raw samples had higher organic carbon levels and average turbidity compared to DC pre-UV (DC Raw TOC = 9.19 mg/L, turbidity = 3.52 NTU; DC pre-UV TOC = 4.30 mg/L, turbidity = 0.51 NTU). This suggests that treatment in DCWTP (coagulation + flocculation + DAF system) resulted in a reduction of conditions that cause UV-resistance. The PSD was also measured to explore possible relationships between size and the obtained results. Two peaks were observed in PSD by volume figures of DC raw water at 0.69 and 5.17 μm, while in DC pre-UV samples, only one peak at 4.95 μm was reported. Data suggested that the treatment applied to DC raw removed the portion of particles smaller than 1 μm. The remaining portion of particles within the size range of 2–6 μm would carry over to the disinfection stage. It has been found by previous studies that UV disinfection efficacy is linked to particle size (Winward *et al.* 2008). Therefore, it is possible that the DAF process removes particulates and small colloids that could interfere with disinfection and result in better UV disinfection and a lower level of tailing.

In previous research by Farrell *et al.* (2018), the relationship between turbidity levels and UV inactivation of *E. coli* and *E. faecalis* was studied. Parallel results were observed where a lower disinfection rate of microorganisms was reported in samples with higher turbidity levels due to increased potential of aggregation and decreased UVT (Farrell *et al.* 2018). It is suggested that along with turbidity, other factors could control the behavior of UV disinfection. Comparison of 82 and 18% of β in two less turbid water samples, DC pre-UV (average turbidity of 0.38 ± 0.09 NTU) and MH pre-UV (average turbidity of 0.61 ± 0.33 NTU), respectively, implies that samples with similar turbidities have shown significantly different responses. ($p < 0.05$ in all three parameters).

It is notable that the initial inactivation slope, k_1, is higher than the secondary inactivation slope k_2, in all cases. It indicates that inactivation occurs at a higher rate for the portion of free-floating microorganisms than for associated microorganisms. This is in agreement with observations (Tan *et al.* 2017), where the same parameters were calculated for trickling filter and activated sludge flocs in three different size fractions. Higher concentrations of particulate matter enhance the chance of microorganisms becoming enmeshed into flocs or shielded by particles. Thus, it can be seen that the difference between k_1 and k_2 is more pronounced in DC raw water than in less turbid samples (DC and MH pre-UV). This is hypothesized due to a lower ratio of non-associated microorganisms in DC raw that become inactivated within a short period. k_1 and k_2 values are significantly different in each sample type ($p < 0.05$). There is no significant difference between k_1 values for each sample type ($p = 0.6$). This supports the idea that the first part of the inactivation curve is associated with free-floating organisms and the response should be independent of water quality. However, k_2 values are different from one another and could be associated directly with water quality. The higher k_2 values are associated with two raw water samples (DC raw and MH pre-UV) with higher inactivation. DC pre-UV with the lowest k_2 value indicates the highest particle–microorganism association, thus the most UV-resistant water sample. The differences between k values are in accordance with the water quality results and UV disinfection. This may be related to the introduction of coagulants that are specifically intended to aggregate particulate for removal however there may be carry over of either particulate or continued effect of the coagulant up to the point of UV disinfection. It can be concluded that the behavior of UV disinfection in the presence of different particles is complex and highly dependent on several water quality conditions that cannot be described with a single indicator such as turbidity or UVT.

Table 2 | UV disinfection model parameters for water samples and control experiments, the error reported as standard deviation between sampling days, $n = 8$–10, ($R^2 > 0.99$ for model fit in all cases)

Sample ID	β	k_1 (cm²/mJ)	k_2 (cm²/mJ)
DC raw	0.64 ± 0.11	0.23 ± 0.05	0.14 ± 0.02
DC pre-UV	0.17 ± 0.03	0.20 ± 0.07	0.11 ± 0.04
MH pre-UV	0.82 ± 0.06	0.20 ± 0.09	0.17 ± 0.07

To further investigate relationships between water quality and dose–response, the significance of correlations between the month-to-month values of modeled parameters (β, k_1, k_2) and water quality indicators were calculated. Generally, there was poor consistency of significant relationships, with no singular modeled parameter and water quality indicator showing significant correlation across all water types. For example, significant correlations were observed between k_1 and zeta potential ($p < 0.05$) in DC raw and MH pre-UV samples but not for DC pre-UV samples ($p = 0.46$). The month-to-month inconsistency further suggests that dose–response in unfiltered waters can be highly variable and conventional water quality indicators are not necessarily strong indicators of expected performance. Variability in this study also suggests that future work using controlled synthetic water samples where individual parameters can be varied independently would help elucidate potential relationships between water quality and UV performance in unfiltered waters. Correlation and statistical results are provided in Supplementary Material, Table S1.

CONCLUSION

This work aimed to provide guidance for drinking water treatment plants applying UV disinfection to unfiltered water and help outline criteria for quality characteristics of unfiltered systems that may impact UV disinfection. The UV disinfection response could not be correlated to the conventional treatment indicators such as turbidity, TOC, and UV adsorption at 254 nm. In previous studies, microorganism protection against UV disinfection has been shown by particles with enmeshment or attachment mechanisms. The results of this study supported the theory that even in high-quality unfiltered water supplies (turbidity less than 1 NTU), particulates with more neutral surface charges could offer significant protection to microorganisms from UV light. In the design of experiments, samples were taken directly from two drinking water treatment facilities. Therefore, control over the tested conditions was limited, and reliable particle size data were not available in this case. Also, there is potential for cross-correlations between zeta potential and other parameters that could be considered in future studies. Additionally, the use of a surrogate measure (MS2) when *Cryptosporidium* inactivation is the true target should be noted.

The effect of water quality on the tailing of UV disinfection kinetics of unfiltered water supplies was also investigated. It was shown that zeta potential had a more significant impact on tailing degree than turbidity and UVA. Water samples with the same turbidity and zeta potential of −11 and −21 mV had about 82 and 17% UV-resistant microorganisms, respectively. A higher level of tailing is assumed to be the consequence of more UV-resistant microorganisms hence more potential of coupling with particles and shielding effect. Observing two water sources with different zeta potentials (−18 and −21 mV at pH 7.2) and different tailing levels (DC and MH pre-UV samples) confirms that the tailing is attributed to the average surface charge. Tailing was also found to be dependent on the pre-treatment. Particles after coagulation and DAF (DC pre-UV) had a lower tailing effect than non-treated water from the same source (DC raw) with a more positive average surface charge.

The observed results suggest a uniform turbidity level or UVA/UVT is not, by themselves, appropriate performance indicator for unfiltered UV disinfection performance. The poor representation of dose–response using these indicators is more pronounced at higher UV doses (>30 mJ/cm^2), and water quality effects are less influential at low doses. The composition of turbidity-causing materials or particulates may be the controlling factor that further needs to be investigated for various microorganisms. Although the UV efficiency is highly source-dependent and risk-based, to reduce the public health risks, based on the results, pre-treatment should be considered even for high-quality surface waters subject to pathogenic contamination and water quality characterization in addition to turbidity and UVA/UVT is needed for accurate assessment of UV disinfection potentials.

ACKNOWLEDGEMENTS

This work was funded by the Natural Sciences and Engineering Research Council of Canada (NSERC) Alliance program and the Regional District of North Okanagan. We would like to thank the personnel at the Regional District of North Okanagan including Zee Marcolin, Tricia Brett, Dustin Heidt, and Taylor Dufaut as well as Stephen Horsman with WSP for their support.

DATA AVAILABILITY STATEMENT

All relevant data are included in the paper or its Supplementary Information.

CONFLICT OF INTEREST

The authors declare there is no conflict.

REFERENCES

Bhullar, M. S., Patras, A., Kilonzo-Nthenge, A., Pokharel, B. & Sasges, M. 2019 Ultraviolet inactivation of bacteria and model viruses in coconut water using a collimated beam system. *Food Science and Technology International* **25** (7), 562–572. https://doi.org/10.1177/1082013219843395.

Cantwell, R. E. & Hofmann, R. 2008 Inactivation of indigenous coliform bacteria in unfiltered surface water by ultraviolet light. *Water Research* **42** (10–11), 2729–2735. https://doi.org/10.1016/j.watres.2008.02.002.

Cantwell, R. E. & Hofmann, R. 2011 Ultraviolet absorption properties of suspended particulate matter in untreated surface waters. *Water Research* **45** (3), 1322–1328. https://doi.org/10.1016/j.watres.2010.10.020.

Cantwell, R. E., Hofmann, R., Rand, J. L., Devine, P. M. & van der Marck, M. 2010 Case study of particle-related UV shielding of microorganisms when disinfecting unfiltered surface water. *Water Quality Research Journal of Canada* **45** (3), 343–351.

Chen, J., Loeb, S. & Kim, J. H. 2017 LED revolution: fundamentals and prospects for UV disinfection applications. *Environmental Science: Water Research and Technology* **3** (2), 188–202. https://doi.org/10.1039/c6ew00241b.

Christensen, J. & Linden, K. G. 2003 How particles affect UV light in the UV disinfection of unfiltered drinking water. *Journal/American Water Works Association* **95** (4), 179–189. https://doi.org/10.1002/j.1551-8833.2003.tb10344.x.

Crittenden, J. C., Trussell, R. R., Hand, D. W., Howe, K. J. & Tchobanoglous, G. 2012 *MWH's Water Treatment: Principles and Design*, 3rd edn. John Wiley & Sons. https://doi.org/10.1002/9781118131473

DeFrancesco, C. & Guéguen, C. 2021 Long-term trends in dissolved organic matter composition and its relation to sea ice in the Canada Basin, Arctic Ocean (2007–2017). *Journal of Geophysical Research: Oceans* **126** (2), e2020JC016578. https://doi.org/10.1029/2020JC016578.

Du, Y., Lu, Y., Roebuck, J. A., Liu, D., Chen, F., Zeng, Q., Xiao, K., He, H., Liu, Z., Zhang, Y. & Jaffé, R. 2021 Direct versus indirect effects of human activities on dissolved organic matter in highly impacted lakes. *Science of The Total Environment* **752**, 141839. https://doi.org/10.1016/j.scitotenv.2020.141839.

Farrell, C., Hassard, F., Jefferson, B., Leziart, T., Nocker, A. & Jarvis, P. 2018 Turbidity composition and the relationship with microbial attachment and UV inactivation efficacy. *Science of the Total Environment* **624**, 638–647. https://doi.org/10.1016/j.scitotenv.2017.12.173.

Garcia, R. D., Diéguez, M. d. C., Gerea, M., Garcia, P. E. & Reissig, M. 2018 Characterisation and reactivity continuum of dissolved organic matter in forested headwater catchments of Andean Patagonia. *Freshwater Biology* **63** (9), 1049–1062. https://doi.org/10.1111/fwb.13114.

Health Canada. 2019 *Guidelines for Canadian Drinking Water Quality Summary Table Prepared by the Federal-Provincial-Territorial Committee on Drinking Water of the Federal-Provincial-Territorial Committee on Health and the Environment March 2006*.

Jutaporn, P., Muenphukhiaw, N., Phungsai, P., Leungprasert, S. & Musikavong, C. 2022 Characterization of DBP precursor removal by magnetic ion exchange resin using spectroscopy and high-resolution mass spectrometry. *Water Research* **217**, 118435. https://doi.org/10.1016/j.watres.2022.118435.

Kollu, K. & Örmeci, B. 2012 Effect of particles and bioflocculation on ultraviolet disinfection of Escherichia coli. *Water Research* **46** (3), 750–760. https://doi.org/10.1016/j.watres.2011.11.046.

Korchef, A. & Touaibi, M. 2020 Effect of pH and temperature on calcium carbonate precipitation by CO2 removal from iron-rich water. *Water and Environment Journal* **34** (3), 331–341.

Kowalczuk, P., Durako, M. J., Young, H., Kahn, A. E., Cooper, W. J. & Gonsior, M. 2009 Characterization of dissolved organic matter fluorescence in the South Atlantic Bight with use of PARAFAC model: interannual variability. *Marine Chemistry* **113** (3), 182–196. https://doi.org/10.1016/j.marchem.2009.01.015.

Lalancette, C., Papineau, I., Payment, P., Dorner, S., Servais, P., Barbeau, B., Di Giovanni, G. D. & Prévost, M. 2014 Changes in Escherichia coli to Cryptosporidium ratios for various fecal pollution sources and drinking water intakes. *Water Research* **55**, 150–161.

Lavonen, E. E., Kothawala, D. N., Tranvik, L. J., Gonsior, M., Schmitt-Kopplin, P. & Köhler, S. J. 2015 Tracking changes in the optical properties and molecular composition of dissolved organic matter during drinking water production. *Water Research* **85**, 286–294. https://doi.org/10.1016/j.watres.2015.08.024.

MaCkey, E. D., Hargy, T. M., Wright, H. B., Malley Jr, J. P. & Cushing, R. S. 2002 Comparing cryptosporidium and MS2 bioassays – implications for UV reactor validation. *Journal-American Water Works Association* **94** (2), 62–69.

Moona, N., Holmes, A., Wünsch, U. J., Pettersson, T. J. R. & Murphy, K. R. 2021 Full-scale manipulation of the empty bed contact time to optimize dissolved organic matter removal by drinking water biofilters. *ACS ES&T Water* **1** (5), 1117–1126. https://doi.org/10.1021/acsestwater.0c00105.

Muoio, R., Caretti, C., Rossi, L., Santianni, D. & Lubello, C. 2020 Water safety plans and risk assessment: a novel procedure applied to treated water turbidity and gastrointestinal diseases. *International Journal of Hygiene and Environmental Health* **223** (1), 281–288.

Murphy, K. R., Stedmon, C. A., Graeber, D. & Bro, R. 2013 Fluorescence spectroscopy and multi-way techniques. PARAFAC. *Analytical Methods* **5** (23), 6557–6566. https://doi.org/10.1039/C3AY41160E.

Murphy, K. R., Bro, R., Stedmon, C. A., 2014a Chemometric Analysis of Organic Matter Fluorescence. In: *Aquatic Organic Matter Fluorescence* (Coble, P., Lead, J., Baker, A., Reynolds, D. M. & Spencer, R. G. M. eds.). Cambridge University Press, pp. 339–375. https://doi.org/10.1017/CBO9781139045452.016

Murphy, K., Stedmon, C., Wenig, P. & Bro, R. 2014b Openfluor– an online spectral library of auto-fluorescence by organic compounds in the environment. *Analytical Methods* **6** (3), 658–661. https://doi.org/10.1039/C3AY41935E.

Osburn, C. L., Boyd, T. J., Montgomery, M. T., Bianchi, T. S., Coffin, R. B. & Paerl, H. W. 2016 Optical proxies for terrestrial dissolved organic matter in estuaries and coastal waters. *Frontiers in Marine Science* **2**. Available from: https://www.frontiersin.org/articles/10.3389/fmars.2015.00127

Parrotta, M. J. & Bekdash, F. 1998 UV disinfection of small ground water supplies. *Journal-American Water Works Association* **90** (2), 71–81.

Peleato, N. M., Sidhu, B. S., Legge, R. L. & Andrews, R. C. 2017 Investigation of ozone and peroxone impacts on natural organic matter character and biofiltration performance using fluorescence spectroscopy. *Chemosphere* **172**, 225–233. https://doi.org/10.1016/j.chemosphere.2016.12.118.

Pirnie, M., Linden, K. G. & Malley Jr., J. P. 2006 Ultraviolet disinfection guidance manual for the final long term 2 enhanced surface water treatment rule. *Environmental Protection* **2** (11), 1–436.

Schafft, M., Wegner, B., Meyer, N., Wolter, C. & Arlinghaus, R. 2021 Ecological impacts of water-based recreational activities on freshwater ecosystems: a global meta-analysis. *Proceedings of the Royal Society B: Biological Sciences* **288** (1959), 20211623. https://doi.org/10.1098/rspb.2021.1623.

Tan, T. C., Azimi, Y. & Farnood, R. R. 2017 Tailing propensity in the ultraviolet disinfection of trickling filter and activated sludgewastewater treatment processes. *Water Science and Technology* **76** (3), 623–632. https://doi.org/10.2166/wst.2017.242.

Templeton, M. R., Andrews, R. C. & Hofmann, R. 2008 Particle-associated viruses in water: impacts on disinfection processes. *Critical Reviews in Environmental Science and Technology* **38** (3), 137–164. https://doi.org/10.1080/10643380601174764.

USEPA 2004 TL, R. T. Comprehensive Surface Water Treatment Rules Quick Reference Guide: Systems Using Conventional or Direct Filtration.

Winward, G. P., Avery, L. M., Stephenson, T. & Jefferson, B. 2008 Ultraviolet (UV) disinfection of grey water: particle size effects. *Environmental Technology* **29** (2), 235–244.

Wright, H., Heath, M. & Bandy, J. 2011 Yikes! What the UVDGM does not address on UV disinfection. *Paper Presente at the (1) Paper Presented at the IOA/IUVA World Congress, Paris, France*.

Zimmer, J. L. & Slawson, R. M. 2002 Potential repair of Escherichia coli DNA following exposure to UV radiation from both medium-and low-pressure UV sources used in drinking water treatment. *Applied and Environmental Microbiology* **68** (7), 3293–3299.

First received 19 April 2022; accepted in revised form 5 October 2022. Available online 17 October 2022